Available online at www.sciencedirect.com
ScienceDirect
Journal of the European Ceramic Society 27 (2007) 1123–1127
www.elsevier.com/locate/jeurceramsoc

Synthesis, microstructure and dielectric properties of antimony-doped strontium titanate ceramics

Adelina Ianculescu [a,*], Ana Brăileanu [b], Georgeta Voicu [a]

[a] *Department of Oxide Materials Science and Engineering, University "Politehnica" Bucharest, 1-7 Gh. Polizu, P.O. Box 12-134, 011061 Bucharest, Romania*
[b] *Institute of Physical Chemistry, "I.G. Murgulescu" of the Romanian Academy, 202 Spl. Independenţei, 060021 Bucharest, Romania*

Available online 13 June 2006

Abstract

Ceramics of $SrTi_{1-x}Sb_xO_3$ ($0 \leq x \leq 0.015$) composition were prepared by solid state reaction. Samples were obtained after sintering in air at 1300 and 1400 °C, respectively, with a soaking time of 3 h. Even at 1000 °C, XRD data show single phase compositions for all samples studied. Above a critical Sb proportion ($x = 0.0075$) the microstructure changes and an abnormal grain growth process starts to occur. Besides, electrical measurements performed at 500 Hz frequency revealed that the dielectric losses start to decrease and the interfacial polarization increases, leading to the increase of the overall effective permittivity, up to a maximum value of ~4500 for $x = 0.01$. The microstructure feature mentioned, as well as the dielectric behaviour are correlated with the change of the supplementary charge compensation induced by Sb^{5+} donor dopant, from an electronic mechanism toward an ionic (by Sr vacancies) one.

Keywords: Defects; Grain size; Microstructure; Dielectric properties; $SrTiO_3$

1. Introduction

$SrTiO_3$ is one of the widely used materials in the electronic ceramic industry as semiconductor material at high temperatures or as dielectric material for internal boundary layer capacitors (IBLC), due to its high dielectric constant and excellent stability with temperature and applied voltage.[1–3]

Donor-type dopants are often added in order to improve the electrical properties of $SrTiO_3$-based ceramics both through changes in defect structure of the perovskite lattice as well as in microstructure of the obtained ceramics.[4–9]

In the present study, the formation and the characteristics of undoped and Sb-doped strontium titanate ceramics were studied as a function of Sb dopant concentration.

2. Experimental

2.1. Samples preparation

Samples with the compositions listed in Table 1 were prepared by classical ceramic method from high purity oxides and carbonates: TiO_2 (Merck), Sb_2O_3 (Merck) and $SrCO_3$ (Fluka), by a wet homogenization technique in isopropyl alcohol.

The initial mixtures were used as powdered samples for non-isothermal investigations. For isothermal investigations, the mixtures were shaped by uniaxial pressing at 160 MPa into pellets of 20 mm diameter and ~3 mm thickness. The pellets were thermally treated in air in the 1000–1400 °C temperature range with 3 h plateau.

2.2. Samples characterization

In order to study the changes which occur during thermal treatments, thermal analyses (TG/DTG and DTA) of the mixtures mentioned were performed up to 1300 °C, in static air atmosphere, with α-Al_2O_3 as reference at a heating rate of 7.5 °C min^{-1}. A MOM Budapest type Paulik–Paulik–Erdey derivatograph OD-103 was used.

Phase composition evolution in isothermal conditions was investigated by X-ray diffraction, by means of a Shimadzu XRD 600 diffractometer.

The microstructure of the samples was examined by scanning electron microscopy, using a Hitachi S2600N equipment.

To estimate the electric behaviour of the sintered materials, electrical measurements of capacitance and dielectric losses

* Corresponding author. Tel.: +40 21 4023848; fax: +40 21 3181010.
E-mail address: a.ianculescu@rdslink.ro (A. Ianculescu).

0955-2219/$ – see front matter © 2006 Elsevier Ltd. All rights reserved.
doi:10.1016/j.jeurceramsoc.2006.05.042

Table 1
Composition of the mixtures investigated

Mixture	Composition
1	$SrTiO_3$
2	$SrTi_{0.9975}Sb_{0.0025}O_3$
3	$SrTi_{0.995}Sb_{0.005}O_3$
4	$SrTi_{0.9925}Sb_{0.0075}O_3$
5	$SrTi_{0.99}Sb_{0.01}O_3$
6	$SrTi_{0.985}Sb_{0.015}O_3$

were performed at room temperature and at 500 Hz frequency, using a Hewlett Packard 4284 A LCR-meter.

3. Results and discussion

Thermal analysis of the raw materials points up specific effects only for $SrCO_3$, for which DTA curve shows two endothermic effects: the first one at 932 °C, corresponding to orthorhombic → hexagonal transformation[10] and the second one at 1027 °C, accompanied by a significant mass loss on the TG curve, due to the $SrCO_3$ decomposition.

For all mixtures, DTA curves show the thermal effects specific for $SrCO_3$ but weaker and shifted to lower temperatures. The shift of the decomposition temperature to lower values is characteristic for carbonated systems in the presence of cations with acid character such as Ti^{4+}. For mixture 1 (pure $SrCO_3$), the second effect is, in fact, the result of two antagonistic effects, corresponding to two simultaneous processes: an endothermic decarbonation and an exothermic formation of strontium metatitanate $SrTiO_3$, according to the reaction (1):

$$SrCO_3 + TiO_2 \rightarrow SrTiO_3 + CO_2 \uparrow \quad (1)$$

In case of the mixture 6, with maximum Sb dopant, (Fig. 1) the decomposition occurs simultaneous with the solid solution formation in a wide temperature range (800–1000 °C), hiding the $Sb^{3+} \rightarrow Sb^{5+}$ oxidation. The reaction which occurs in this temperature range could be written as:

$$SrCO_3 + (1-x)TiO_2 + \frac{x}{2}Sb_2O_3 + \frac{x}{2}O_2 \rightarrow SrTi_{1-x}Sb_xO_3 + CO_2 \uparrow \quad (2)$$

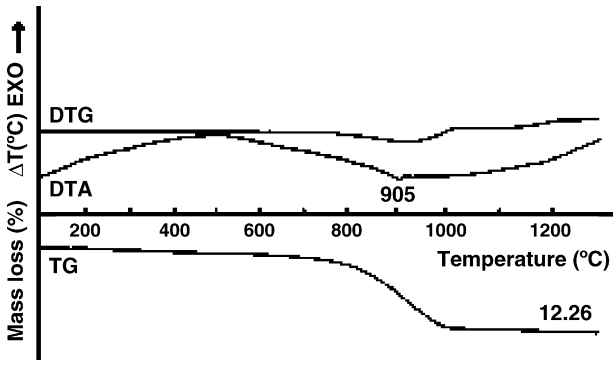

Fig. 1. Thermal analyses curves for the composition 6, $SrTi_{0.985}Sb_{0.015}O_3$, with the highest Sb content.

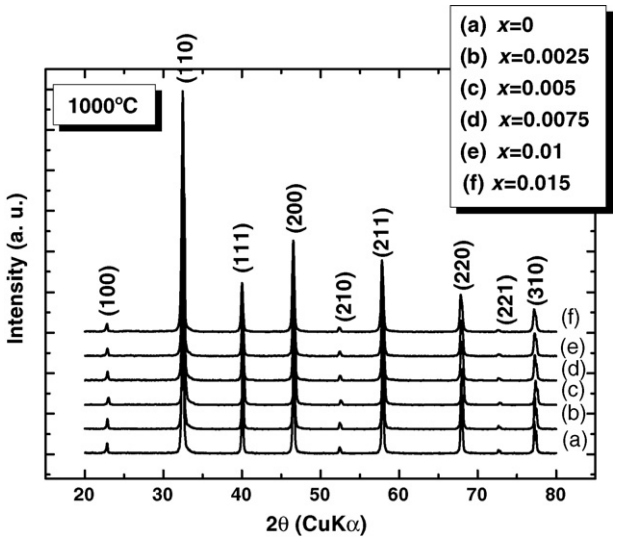

Fig. 2. X-ray diffraction patterns of the $SrTi_{1-x}Sb_xO_3$ solid solutions, isothermally treated at 1000 °C/3 h.

X-ray diffraction measurements performed for the mixtures isothermally treated at various temperatures 1000, 1100 and 1200 °C sustain thermal analysis data.

Even at 1000 °C, XRD data point out, for all six compositions studied, the presence of the characteristic diffraction maxima of the single phase $SrTi_{1-x}Sb_xO_3$ solid solution, which has the ideal perovskite structure of $SrTiO_3$ (Fig. 2).

The increase of Sb concentration determines no phase composition changes, proving that the isomorphy limit of antimony in $SrTiO_3$ lattice was not reached yet. Sb, incorporated as Sb^{3+} (Sb_2O_3), oxidizes to Sb^{5+} during the thermal treatment and replaces Ti^{4+} in the perovskite lattice, due to the small difference between ionic radii of the substitute ($r_{Ti}^{4+} = 0.68$ Å) and of the substituent ($r_{Sb}^{5+} = 0.62$ Å), in the studied concentration range. These results are in agreement with those reported by Burn and Neirman.[11]

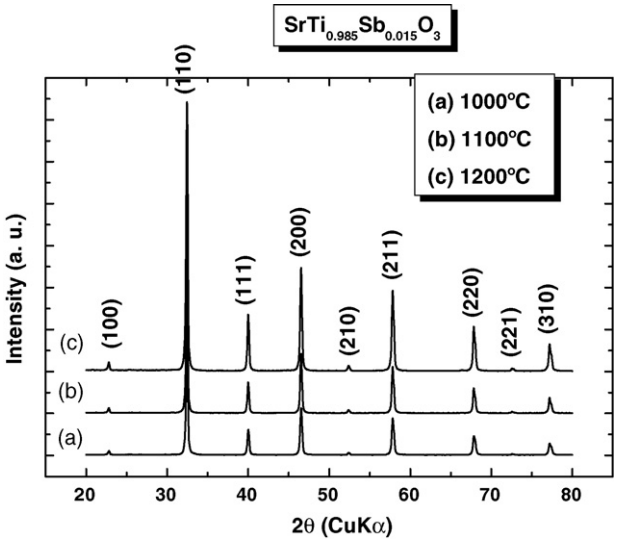

Fig. 3. X-ray diffraction patterns of the composition 6, $SrTi_{0.985}Sb_{0.015}O_3$, against temperature.

With the temperature rise, for all six mixtures a more pronounced crystallinity reflected in the increase of the characteristic diffraction peaks intensities of the solid solutions was observed. Fig. 3 shows the X-ray diffraction patterns for the composition 6 (with the highest Sb content of $x = 0.015$) as a function of the temperature.

SEM analyses, performed on samples sintered at 1400 °C reveal for pure $SrTiO_3$ a dense microstructure, consisting of homogeneously distributed grains with the main size of 10 μm and some intergranular pores (Fig. 4(a)).

The small Sb proportion in $SbTi_{0.995}Sb_{0.005}O_3$ composition (Fig. 4(c)) does not determine essential changes of the

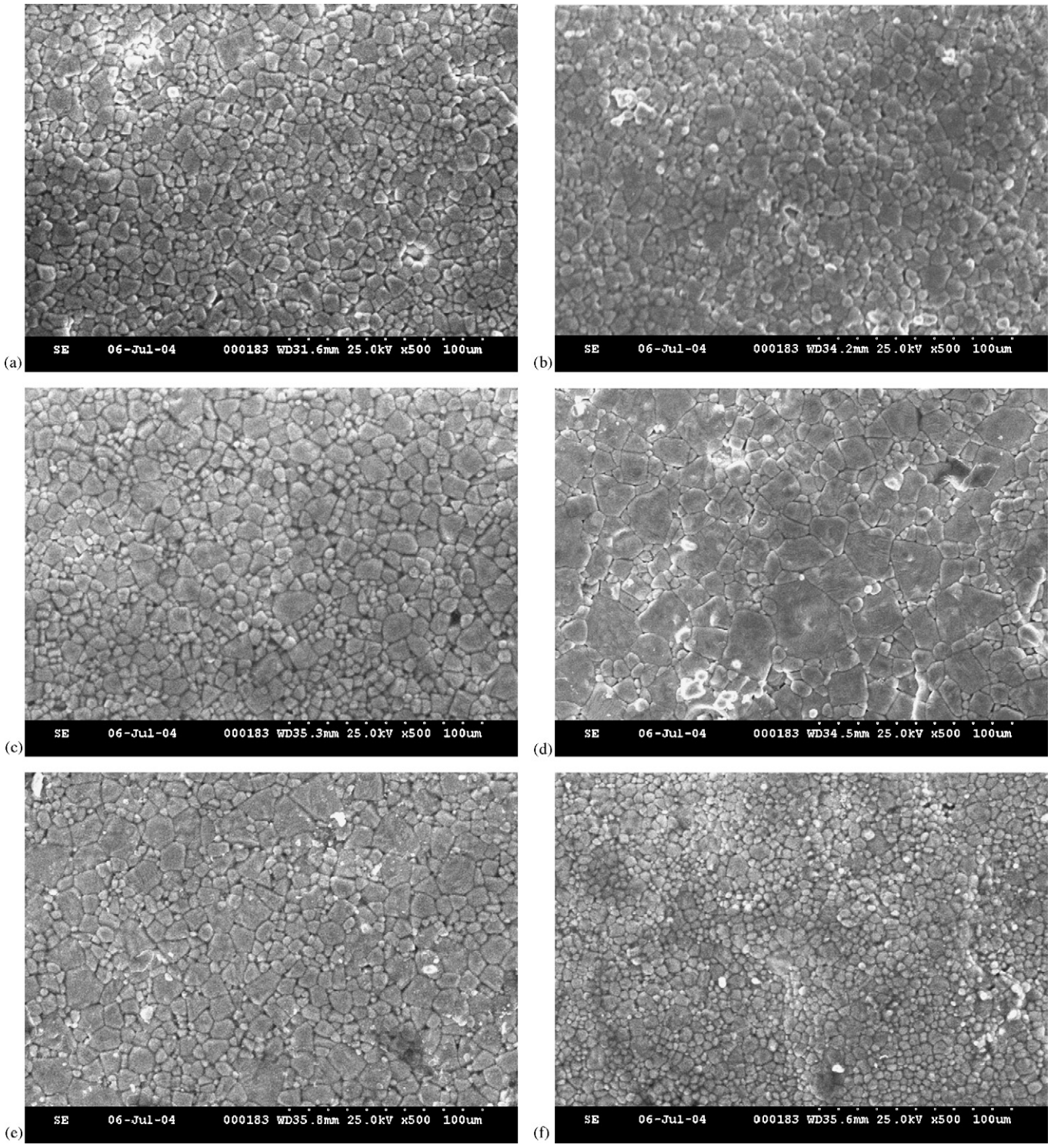

Fig. 4. SEM micrographs of the compositions sintered at 1400 °C: (a) $SrTiO_3$; (b) $SrTi_{0.9975}Sb_{0.0025}O_3$; (c) $SrTi_{0.995}Sb_{0.005}O_3$; (d) $SrTi_{0.9925}Sb_{0.0075}O_3$; (e) $SrTi_{0.99}Sb_{0.01}O_3$; (f) $SrTi_{0.985}Sb_{0.015}O_3$.

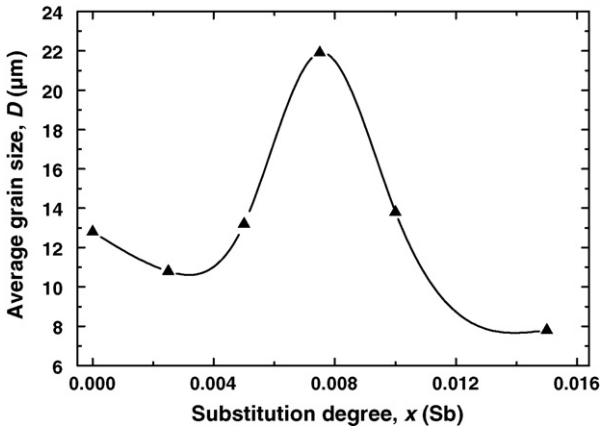

Fig. 5. The average grain size evolution vs. the antimony content for samples sintered at 1400 °C.

microstructure. The increase of Sb concentration up to the critical value of $x = 0.0075$ determines an abnormal growth of the grains. Thus, for the solid solution $SrTi_{0.9925}Sb_{0.0075}O_3$ (Fig. 4(d)), a non-homogeneous microstructure, consisting both of small grains with $\phi = 5\,\mu m$ and very large grains with $\phi = 20\,\mu m$ can be observed, although the material is very well densified, with a minimum intergranular porosity. For the ceramic with the highest Sb proportion, $SrTi_{0.985}Sb_{0.015}O_3$ (Fig. 4(f)), another spectacular change of the microstructure can be remarked. The larger grains vanish totally and the microstructure is homogeneous, consisting of ~5 μm grains. SEM micrograph of this composition sintered at 1400 °C shows a total lack of the porosity and perfect triple grain junctions. Fig. 5 shows the dependence of the average grain size on the antimony content. These microstructure features were reported also by Cho and Johnson[8] for their Nb-doped $SrTiO_3$ samples, where the critical dopant concentration was strongly influenced by the Sr/(Ti + Nb) ratio.

The variations of the relative permittivity and of the dielectric loss for the samples sintered, as a function of Sb proportion, are presented in Fig. 6.

For the composition with $0 < x \leq 0.0075$, the increase of the Sb concentration leads to the increase of the charge carrier concentration (electrons) resulted in the partially reduction of Ti^{4+} to Ti^{3+}, in order to compensate the supplementary charge induced by the donor dopant, according to the reaction (3):

$$SrO + (1-x)TiO_2 + \frac{x}{2}Sb_2O_5 \rightarrow SrTi_{1-2x}Ti'_xSb_x^{\bullet}O_3 + \frac{x}{4}O_2\uparrow \quad (3)$$

As a consequence, the maximum value of the dielectric loss is recorded for a Sb proportion of $x = 0.0025$. Over the critical value ($x = 0.0075$), the compensation mechanism starts to modify with the increase of the proportion of cation vacancies generated at the grain boundary, in order to maintain the electroneutrality of the lattice (Eqs. (4) and (5)).

$$SrO + (1-x)TiO_2 + \frac{x}{2}Sb_2O_5 \rightarrow Sr_{1-x/2}(V''_{Sr})_{x/2}Ti_{1-x}Sb_x^{\bullet}O_3 + \frac{x}{2}SrO \quad (4)$$

$$SrO + (1-x)TiO_2 + \frac{x}{2}Sb_2O_5 \rightarrow SrTi_{1-5x/4}(V''''_{Ti})_{x/4}Sb_x^{\bullet}O_3 + \frac{x}{4}TiO_2 \quad (5)$$

Consequently, the dielectric losses decrease (from $\sim 10^{-2}$ to $\sim 10^{-3}$) and the interfacial polarization increases, leading to an increase of the overall effective permittivity from ~750 up to a maximum value of ~4500 for $x = 0.01$. A similar permittivity evolution against the dopant concentration was found by Chen and Zhi[5] for their lanthanum-doped $SrTiO_3$ solid solutions.

For the Sb proportion of $x > 0.01$, the cation vacancy concentration increases continuously. These defects tend to distribute uniformly in the whole grain bulk. As a result, the interfacial polarization mechanism starts to be cancelled and the dielectric permittivity decreases again to ~750. This phenomenon is accompanied by the drastic diminution of the average grain size, as a consequence of the inhibiting effect of the donor dopant on the grain growth process. This involves the porosity increase and therefore higher dielectric losses were recorded. Because of the pronounced decrease of the average grain size, the grain boundary layers depleted in charge carriers (electrons) and rich in cation vacancies, tend to exhibit similar thickness with the grain size. Therefore, homogeneous grains from the point of view of the defect distribution were obtained, which leads to lower relative permittivity values.

Theoretically, both Sr and Ti vacancies could compensate the supplementary charge induced by Sb. The Sr vacancies are much more thermodynamically favourable as compensating defects, in comparison with Ti vacancies in the octahedral interstices. This assumption is sustained by the lack of a Ti-rich secondary phase, which is expected to result according to Eq. (5) if the Ti vacancies are the compensating defects. The lack of a Sr-rich secondary phase, according to Eq. (4), can be explained in terms of a possible supplementary Sr incorporation into the perovskite structure, by a Ruddlesden–Popper structural accommodation, which involves a superstructure formation consisting of SrO layers incorporated at ~30 perovskite layers.[5] Therefore, in accord with our X-ray diffraction data we concluded that for higher Sb

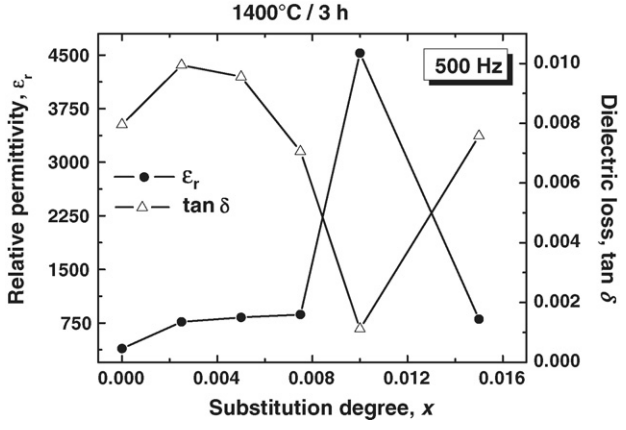

Fig. 6. The evolution of the relative permittivity and dielectric loss against the Sb content at 1400 °C.

concentrations ($x > 0.0075$), strontium vacancies are the most probable compensating defects in antimony-doped $SrTiO_3$.

4. Conclusions

Even at 1000 °C, XRD data point out, for all six compositions studied, the presence of the characteristic diffraction maxima of the single phase $SrTi_{1-x}Sb_xO_3$ solid solution, which has the ideal perovskite structure of $SrTiO_3$.

The microstructure of the ceramics is influenced by the Sb proportion. Pure $SrTiO_3$ has a dense microstructure, which is not much affected by the introduction of small Sb amounts ($x < 0.0075$). For the composition with the antimony content of $x = 0.0075$, an abnormal grain growth process occurs, leading to a heterogeneous microstructure. Over this Sb proportion the average grain size starts to decrease, so that for the ceramics with the highest antimony content, a very homogeneous microstructure consisting of small grains can be noticed.

This microstructure feature is correlated with the change of compensation mechanism of the supplementary charge induced by the Sb^{5+} donor dopant. Thus, below a critical antimony concentration ($x \leq 0.0075$) the compensating defects are the electrons resulted in the Ti^{4+} toward Ti^{3+} partially reduction, whereas over this concentration value, a strontium vacancy compensation mechanism was assumed as the most probable.

Above this critical Sb concentration the dielectric losses start to decrease and the interfacial polarization increases, leading to the increase of the overall effective permittivity. Therefore, for the sample with the Sb content of $x = 0.01$, the permittivity jumped massively to 4500, unlike the other antimony-doped compositions which have a roughly similar relative permittivity value (∼750).

References

1. Chan, N. H., Sharma, R. K. and Smyth, D. M., Non-stoichiometry in $SrTiO_3$. *J. Electrochem. Soc.*, 1981, **128**, 1762–1769.
2. Moos, R. and Härdtl, K. H., Defect chemistry of donor-doped and undoped strontium titanate ceramics between 1000 and 1400 °C. *J. Am. Ceram. Soc.*, 1997, **80**, 2549–2562.
3. Waser, R., Electronic properties of grain boundaries in $SrTiO_3$ and $BaTiO_3$ ceramics. *Solid State Ionics*, 1995, **95**, 89–99.
4. Balachandran, U. and Eror, N. G., Electrical conductivity in lanthanum-doped strontium titanate. *J. Electrochem. Soc.*, 1982, **129**, 1021–1026.
5. Chen, A. and Zhi, Y., Dielectric properties and defect structure in lanthanum-doped $SrTiO_3$ ceramics. *J. Appl. Phys.*, 1992, **71**, 6025–6028.
6. Chen, A. and Zhi, Y., Dielectric properties and complex defect in $(Sr_{1-x}Bi_{2/3x})TiO_3$ ceramics. *J. Appl. Phys.*, 1992, **71**, 4451–4454.
7. Inoue, T., Seki, N., Kamimae, J.-I., Eguchi, K. and Arai, H., The conduction mechanism and defect structure of acceptor- and donor-doped $SrTiO_3$. *Solid State Ionics*, 1991, **48**, 283–288.
8. Cho, S. G. and Johnson, P. F., Evolution of the microstructure of undoped and Nb-doped $SrTiO_3$. *J. Mater. Sci.*, 1994, **29**, 4866–4874.
9. Bae, C., Park, J.-G., Kim, Y.-H. and Jeon, H. J., Abnormal grain growth of niobium-doped strontium titanate ceramics. *J. Am. Ceram. Soc.*, 1998, **81**, 3005–3010.
10. Ianculescu, A., Brăileanu, A., Zaharescu, M., Guillemet, S., Pasuk, I., Madarász, J. *et al.*, Formation and properties of some Nb-doped $SrTiO_3$ solid solutions. *J. Therm. Anal. Cal.*, 2003, **72**, 173–180.
11. Burn, I. and Neirman, S., Dielectric properties of donor-doped polycrystalline $SrTiO_3$. *J. Mater. Sci.*, 1982, **17**, 3510–3524.